

Nuclear bound states of ω mesons ^{*}

F. Klingl, T. Waas[†] and W. Weise
 Physik-Department
 Technische Universität München
 D-85747 Garching, Germany

September 26, 2018

Abstract

Models based on chiral $SU(3)_L \otimes SU(3)_R$ symmetry and vector meson dominance suggest an attractive potential for the ω -meson in a nuclear medium. We discuss the feasibility of producing nuclear bound states of ω -mesons using $(d, {}^3He)$ and pion induced reactions on selected nuclear targets.

1 Introduction

QCD with massless u -, d - and s -quarks has a chiral $SU(3)_L \otimes SU(3)_R$ symmetry which is known to be spontaneously broken. The scalar density of quarks develops a non-vanishing ground state expectation value, the chiral condensate $\langle \bar{q}q \rangle$. The Hellmann-Feynman theorem suggests that the magnitude of this condensate decreases with increasing baryon density [1] at a rate determined, to linear order in density, by the pion-nucleon sigma term. At the density of normal nuclear matter, $\rho = \rho_0 = 0.17 \text{ fm}^{-3}$, the condensate changes from its value at $\rho = 0$ by roughly 30 %.

Spontaneously broken chiral symmetry is expected to be restored at high temperatures and possibly at very high baryon densities. At that point the masses of the ($J^\pi = 1^-$) vector mesons should become degenerate with those of their chiral partners, the ($J^\pi = 1^+$) axial vector mesons. One expects that in-medium vector meson spectra should show traces of this tendency already at moderate densities. In particular, if vector mesons experience a sufficiently strong attractive potential in matter, they could form bound states with ordinary nuclei.

Such attraction was suggested by in-medium QCD sum rules [4] and by a simple scaling hypothesis (“Brown-Rho scaling”, [5]). More detailed analysis [6, 7] has revealed that the ρ meson is probably not a good signal since its large vacuum width of about 150 MeV will be further magnified by in-medium reactions. In contrast, the ω meson appears to be a better candidate [7]. Its small width in free space (about 8 MeV) might increase by a

^{*}Work supported in part by GSI and BMBF

[†]Present adress: Siemens AG, D-81359 München

factor of five or so in nuclear matter, but this is still within reasonable limits so that the ω meson has a chance to survive as a quasi-particle in the nuclear medium. At the same time the calculations suggest that its in-medium mass is shifted downward by about 15% at $\rho = \rho_0$ [7], an amount consistent with the original QCD sum rule analysis [4]. While much of the recent activities have focused on possible in-medium modifications of vector mesons spectra in the context of ultra-relativistic heavy-ion collisions, it is certainly useful to explore such effects under less extreme, better controlled conditions: hence the quest for possible ω meson (quasi-) bound states in ordinary nuclei. Similar questions have been raised in refs. [8, 9].

Our paper proceeds as follows. In section 2 we present an update of the ωN interaction and the in-medium spectrum of the ω meson. Section 3 focuses on the ω -nuclear optical potential and its quasi-bound states. In section 4 we explore possible mechanisms for producing such states: the $(d, {}^3\text{He})$ reaction and pion-induced ω production. Concluding remarks follow in section 5.

2 Update on the ω meson self-energy in nuclear matter

The framework of our discussions is an effective Lagrangian, based on chiral $\text{SU}(3)_L \otimes \text{SU}(3)_R$ symmetry, which incorporates the octet of pseudoscalar Goldstone bosons (pions, kaons, ...), baryons and vector mesons [10, 7]. It specifically includes anomalous couplings of the ω meson related to the Wess-Zumino term.

In ref. [7] we have calculated in-medium spectra of ρ , ω and ϕ mesons using this framework. For the ω meson, the basic input is the ω -nucleon amplitude in free space, $T_{\omega N}(E)$, as a function of energy E at zero three-momentum, $\vec{q} = 0$. Restricting the discussion to $\vec{q} = 0$ is justified since ω mesons bound to nuclei will have small average momenta, $\langle \vec{q}^2 \rangle \ll m_\omega^2$.

In comparison with our previous results for $T_{\omega N}$ presented in ref. [7], improvements have recently been made by more rigorous inclusion of constraints from the measured $\pi^- p \rightarrow \omega n$ cross section [11]. We have also examined uncertainties arising from the incompletely known (off-shell) behaviour of $T_{\omega N}(E)$ at large E . We have performed further calculations of $T_{\omega N}$ as specified in ref. [7] where all the technical details can be found, but using two different input sets, A and B [12]. These sets differ in their treatment of $\omega N \rightarrow \pi\pi N$ processes involving intermediate ρN states, as illustrated in Fig. 1. Set A includes the box diagrams, Figs. 1a and b. Set B incorporates in addition the diagram, Fig. 1c, in which the ρN interaction vertex has large tensor coupling ($\kappa_\rho \simeq 6$). Fig. 2a shows the real and imaginary parts of $T_{\omega N}(E, \vec{q} = 0)$ calculated with sets A and B, respectively. The imaginary parts are evaluated as described in ref. [7] (choosing the sign of the $\omega\rho\pi$ coupling to be consistent with the constraints from $\pi^- p \rightarrow \omega n$), and the real parts are obtained using the dispersion relation (2). The differences between the solid and dashed curves (sets A vs. B) give a rough impression of the model dependence of $T_{\omega N}$ at high energy due to uncertainties in the $\omega N \leftrightarrow \rho N$ coupled channel dynamics.

We note that $T_{\omega N}$ is strongly energy dependent, its real part changing from repulsion at $E = 0$ to attraction at $E \sim m_\omega$. The imaginary part rises quickly at energies $E > m_\omega$.

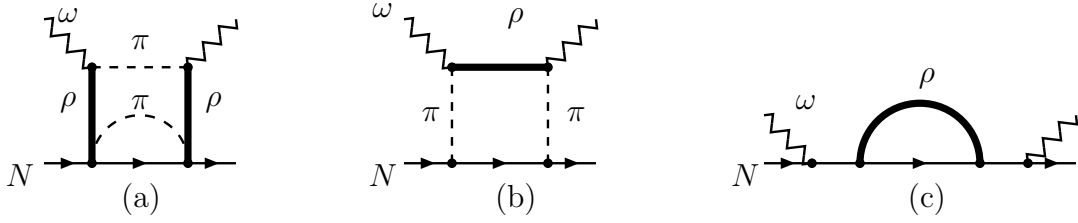


Figure 1:

Contributions to $T_{\omega N}$ involving the $\omega N \rightarrow \pi\pi N$ reaction channel. The thin solid line represents the nucleon. The ρ meson propagators in diagrams (b) and (c) include $\rho \rightarrow \pi\pi$ decay. Set A incorporates diagrams (a) and (b). Set B sums up all three diagrams, also including mixed terms between (b) and (c).

It represents the sum of the $\omega N \rightarrow \pi N$, $\pi\pi N$, etc. reaction channels (see Fig. 2b). The $\omega N \rightarrow \pi\pi N$ channel is actually the prominent one for $E \gtrsim 0.7$ GeV, while the relatively small $\omega N \rightarrow \pi N$ reaction width determines $\text{Im}T_{\omega N}$ at $E \lesssim 0.6$ GeV.

Our calculated effective scattering length (with set A),

$$a_{\omega N} = \frac{M_N}{4\pi(M_N + m_\omega)} T_{\omega N}(E = m_\omega) = (1.6 + i0.3) \text{ fm}, \quad (1)$$

suggests a substantial downward shift of the in-medium ω mass and a moderately increasing width in matter¹. This downward shift comes in large part from 2π -exchange processes such as Fig. 1(b) which, at the same time, have large inelasticities from $\omega N \rightarrow \rho N \rightarrow \pi\pi N$.

Remaining uncertainties concern the constant $T_{\omega N}(E = 0)$ which enters into the dispersion relation

$$\text{Re} T_{\omega N}(E) = T_{\omega N}(0) + \frac{E^2}{\pi} \mathcal{P} \int_0^\infty du^2 \frac{\text{Im} T_{\omega N}(u)}{u^2(u^2 - E^2)}, \quad (2)$$

used to derive $\text{Re} T_{\omega N}$ from the calculated $\text{Im} T_{\omega N}$. Vector Meson Dominance (VMD) connects $T_{\omega N}(0)$ with the Thomson limit of the Compton scattering amplitude, so that $T_{\omega N}(0) = -\left(\frac{3g}{2}\right)^2 M_N^{-1}$ with the nucleon mass M_N and the universal vector coupling constant $g = m_\rho/(\sqrt{2}f_\pi) \simeq 5.9$. Deviations from VMD could arise from additional contact terms proportional to $\bar{N}N\omega_\mu\omega^\mu$ in the effective Lagrangian, so that the constant $T_{\omega N}(0)$ remains basically unconstrained.

Nevertheless, a first order estimate for the ω meson mass shift in nuclear matter gives, using eq.(1):

$$\frac{\Delta m_\omega(\rho)}{m_\omega} = -\frac{2\pi\rho}{m_\omega^2} \left(1 + \frac{m_\omega}{M_N}\right) \text{Re} a_{\omega N} \simeq -0.2 \frac{\rho}{\rho_0}, \quad (3)$$

which is consistent with the in-medium QCD sum rule analysis [4, 7]. The in-medium QCD sum rule does not have quantitative predictive power because of uncertainties related

¹Our updated values in eq.(1) are smaller than those in ref. [7] where the $\omega N \rightarrow \pi N$ reaction width had been overestimated. This has now been corrected.

to the treatment of the density dependence of four-quark condensates, but it is still useful for orientation. It provides a model independent consistency test for the first moment of the ω meson spectral distribution [13], in vacuum as well as in nuclear matter.

The detailed evaluation [7] of the in-medium ω meson spectrum involves the self-energy tensor, $\Pi^{\mu\nu}(E, \vec{q}; \rho)$, of the ω meson in nuclear matter at density ρ . For vanishing momentum \vec{q} its longitudinal and transverse parts $\Pi^{(L,T)}(\omega, \vec{q}; \rho)$ coincide, and we introduce

$$\Pi(E; \rho) \equiv -\frac{1}{3}\Pi_{\mu}^{\mu}(E, \vec{q} = 0; \rho) = \Pi^{(T)}(E, \vec{q} = 0; \rho) = \Pi^{(L)}(E, \vec{q} = 0; \rho). \quad (4)$$

At $\rho = 0$, the imaginary part of Π gives the vacuum decay width of the ω meson, and

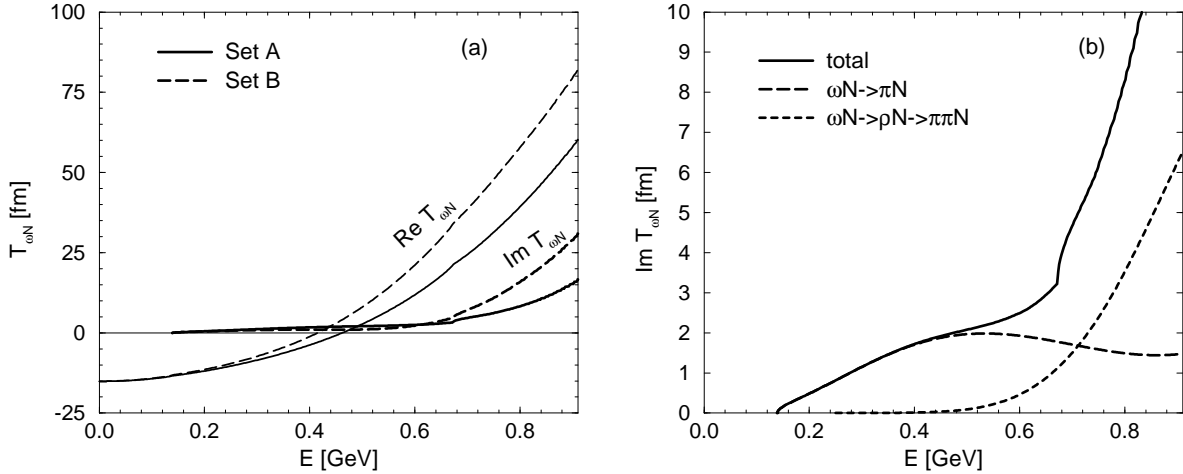


Figure 2: a) Real and imaginary parts of the ωN amplitude $T_{\omega N}(E, \vec{q} = 0)$ calculated with set A (solid) and set B (dashed). For further details see ref. [7].

b) Contributions to $\text{Im}T_{\omega N}(E, \vec{q} = 0)$ from $\omega N \rightarrow \pi N$ and $\omega N \rightarrow \pi\pi N$ reaction channels together with the total result (solid line) for Set A.

its real part is absorbed into the physical free mass m_{ω} . The density dependent part of Π involves the ω -nuclear interaction which is treated to leading order in the density ρ . The in-medium propagator for the ω meson “at rest”, $D_{\omega} = -(E^2 - m_{\omega}^2 - \Pi)^{-1}$, reduces to:

$$D_{\omega}(E, \vec{q} = 0; \rho) = \frac{-1}{E^2 - m_{\omega}^2 + iE\Gamma_{\omega}^{(0)}(E) + \rho T_{\omega N}(E)}, \quad (5)$$

with $\Gamma_{\omega}^{(0)} = 8.4$ MeV at $E = m_{\omega}$ and the complex ωN amplitude $T_{\omega N}$ as given in Fig. 2(a). Note that $\Gamma_{\omega}^{(0)}(E)$ represents the $\omega \rightarrow \pi^+\pi^0\pi^-$ decay and grows even faster with energy E than the 3π phase space.

The spectral distribution $\text{Im}D_{\omega}$ at nuclear matter density $\rho = \rho_0 = 0.17 \text{ fm}^{-3}$ is shown in Fig. 3 in comparison with the vacuum ($\rho = 0$) spectrum. The solid and dashed curves at $\rho = \rho_0$ reflect the model dependence in the calculations. Despite such uncertainties, the following features are clearly visible:

- The ω meson (unlike the ρ meson) is expected to persist as a quasi-particle in nuclear matter when it has a small momentum relative to the surrounding medium.

- The in-medium ω meson mass at $\rho = \rho_0$ is shifted downward by about 15 % from the free m_ω .
- The predicted in-medium ω meson decay width (at resonance) is $\Gamma_{\text{eff}}(\rho = \rho_0) \simeq 40$ MeV, about five times as large as the free width, but still about an order of magnitude smaller than m_ω .

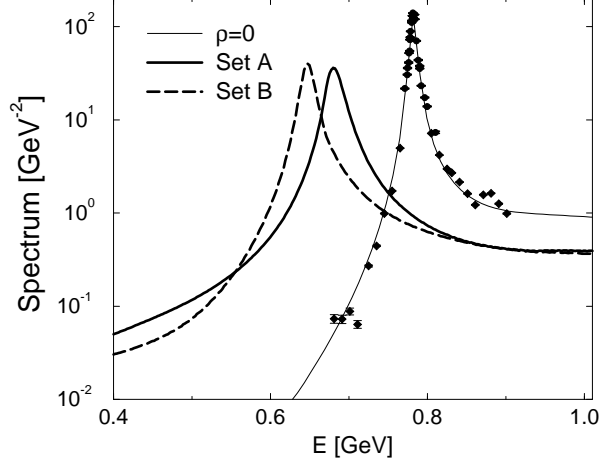


Figure 3: a) Spectral distribution $\text{Im } D_\omega(E, \vec{q} = 0)$ of the ω meson in vacuum (thin line, with data) and in nuclear matter at density $\rho = \rho_0 = 0.17 \text{ fm}^{-3}$, for set A (solid) and set B (dashed). The data points correspond to $e^+e^- \rightarrow \omega \rightarrow 3\pi$ in vacuum [14].

We repeat that our calculated ω spectrum in matter is perfectly consistent with the QCD sum rule analysis [4, 7]. In fact, the first moment of this spectral distribution (which does not depend on the four-quark condensate but only on the gluon and quark condensates together with the first moment of the quark distribution known from deep inelastic lepton-nucleon scattering) follows precisely the trend expected from QCD sum rules [13].

We use our predicted spectrum as basis for the discussion of possible ω meson quasi-bound states. The term “quasi-bound” should indicate that such bound states, if existent, will have short lifetimes due to their hadronic decays, but the widths are not overwhelmingly large according to our calculated $\text{Im}T_{\omega N}$.

nucleus	n	$(\mathcal{E}_{nl}, \Gamma_{nl})$ [MeV]		
		l=0	l=1	l=2
${}^6_\omega He$:	(1)	(-49,32)	(-19,26)	-
${}^{11}_\omega B$:	(1)	(-66,38)	(-40,34)	(-13,30)
	(2)	(-14,26)	-	-
${}^{26}_\omega Mg$:	(1)	(-83,42)	(-64,40)	(-45,40)
	(2)	(-42,38)	(-21,36)	(-1,28)
	(3)	(-2,24)	-	-
${}^{39}_\omega K$:	(1)	(-87,42)	(-74,42)	(-57,42)
	(2)	(-54,40)	(-36,40)	(-17,36)
	(3)	(-16,34)	-	-

Table 1: Complex eigenenergies, $E_{nl} = m_\omega + \mathcal{E}_{nl} - \frac{i}{2}\Gamma_{nl}$, obtained by solving the Klein-Gordon equation (7) with the potential (6) and density (10) using set A as input.

3 The ω -nuclear potential and quasi-bound states

In the local density approximation, the ω meson self-energy (4) can be translated into a complex, energy dependent local potential:

$$\begin{aligned} \Pi(E, \vec{r}) &\equiv 2EU(E, \vec{r}) \\ &= -\text{Re}T_{\omega N}(E)\rho(\vec{r}) - i[ET_{\omega}^{(0)}(E) + \text{Im}T_{\omega N}(E)\rho(\vec{r})]. \end{aligned} \quad (6)$$

Notably, $\text{Re}U$ can reach values of order -100 MeV in the center of nuclei and at the energies in question. Non-local terms proportional to $\vec{\nabla}\rho(\vec{r}) \cdot \vec{\nabla}$ are expected to be less important and will be dropped in the present survey calculation. Given that the longitudinal and transverse parts of the self-energy are the same in the limit $\vec{q} \rightarrow 0$, all four vector components of the ω meson field are described by a single wave function $\phi(\vec{r})$ which satisfies the Klein-Gordon equation

$$\left[E^2 + \vec{\nabla}^2 - m_\omega^2 - \Pi(E, \vec{r}) \right] \phi(\vec{r}) = 0. \quad (7)$$

Quasi-bound ω -nuclear states are defined by self-consistent solutions of eq. (7) at complex energies E_λ for which $\text{Re}E_\lambda < m_\omega$. We introduce

$$\mathcal{E}_\lambda = \text{Re}E_\lambda - m_\omega \quad (8)$$

and refer to $-\mathcal{E}_\lambda$ as the binding energies of these states. Their total decay widths are given by

$$\Gamma_\lambda = -2\text{Im}E_\lambda. \quad (9)$$

For the nuclear density distributions we use two-parameter Fermi profiles

$$\rho(r) = \frac{\mathcal{N}}{1 + e^{(r-R)/a}}, \quad (10)$$

with $R = (1.18A^{\frac{1}{3}} - 0.5)$ fm and $a = 0.5$ fm. The normalization constant \mathcal{N} is determined by $\int d^3r \rho = A$.

In table 1 we summarize the complex eigenenergies found by solving eq.(7) for selected (somewhat unusual) light and medium weight nuclei. The reason for their choice is that these nuclei can be formed in $(d, {}^3\text{He})$ reactions as in the GSI proposal [8]. The calculations have been done with spherically symmetric density distributions (10), so that the quasi-bound ω meson states are labeled by their principal quantum number and their angular momentum, $\lambda = n, l$.

One observes that the attractive potential (6) supports quasi-bound omega meson states even for light nuclei. The examples given in table 1 should be representative for a wider class of nuclei, and we do not expect that detailed nuclear structure effects such as deformations change this picture qualitatively. These quasi-bound states are of course short-lived, with full widths that are generally of similar magnitude as their binding energies. Unless these widths are grossly underestimated, one should be able to see spectral strength at energies below the free ω mass, even if these states may not be resolved individually.

Our predictions in table 1 are in qualitative agreement with the findings of ref. [9]. They differ at a quantitative level since our ω -nuclear potential has the important feature that it is strongly energy dependent. The strength of the attractive real part of our potential tends to grow with increasing energy in the vicinity of $E \simeq m_\omega$, so that it actually supports more quasi-bound states than the potential of ref. [9]. The energies of the lowest ($1s$) states are nevertheless strikingly similar in both calculations. The primary point of our approach is that we can offer an estimate, based on explicit calculations, for the widths of such states with realistic constraints from the prominent ωN reaction channels.

Our intermediate conclusion is the following: if the ω meson mass experiences a downward shift in nuclear matter by 10 – 15% at $\rho = \rho_0$, then this effect should be visible already in ordinary, even light nuclei by the appearance of quasi-bound states.

4 Production of ω -nuclear states

4.1 Transfer reaction

Hayano et al. [8] suggested to produce bound ω states through transfer reactions of the type $d + A \rightarrow {}^3\text{He} + \omega(A - 1)$. Here the incoming deuteron with momentum \vec{p}_d picks up a bound proton in the target nucleus A to form an outgoing ${}^3\text{He}$ together with an ω meson attached to the residual $(A - 1)$ nucleus. The final ${}^3\text{He}$ energy E_{He} and momentum \vec{p}_{He} is measured in forward direction. The basic idea is to minimize the momentum $\vec{q} = \vec{p}_{He} - \vec{p}_d$ transferred to the residual system with its bound ω meson. Energy and momentum conservation implies that such conditions would ideally be met with a deuteron beam of kinetic energy $T_d \simeq 10$ GeV to produce the ω meson at rest. Even for the lower deuteron beam energies available at GSI ($T_d \simeq 4$ GeV) the situation would still be favourable since the momentum transfers would be around $q \sim 0.2$ GeV, well within the range of the typical of nucleon Fermi momentum in the nucleus.

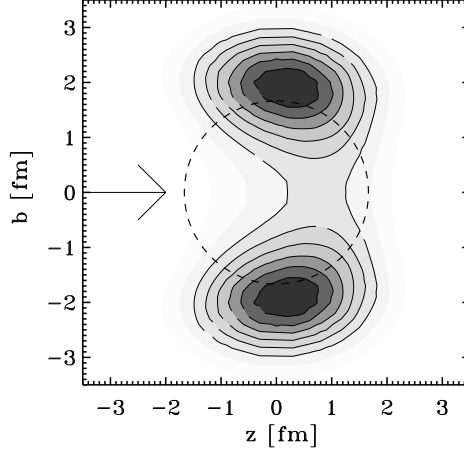


Figure 4: Contour plot of $D(z, b)\rho(r)$ indicating the reaction zone for the $(d, {}^3\text{He})$ process on a typical light target nucleus. The dashed circle indicates the r.m.s radius of the target.

The framework of our calculation is the distorted wave impulse approximation. The $(d, {}^3\text{He})$ differential cross section for ω meson production is written

$$\left(\frac{d^2\sigma_{d+A \rightarrow {}^3\text{He}+\omega(A-1)}}{dE d\Omega} \right)_{\theta=0}^{\text{lab}} = \left(\frac{d\sigma_{d+p \rightarrow {}^3\text{He}+\omega}}{d\Omega} \right)_{\theta=0}^{\text{lab}} S(E). \quad (11)$$

The free cross section $(d\sigma_{d+p \rightarrow {}^3\text{He}+\omega}/d\Omega)$ has been measured at SATURNE [15]. Its value in the lab frame at $T_d \simeq 4 \text{ GeV}$ is approximately $0.5 \mu\text{b/sr}$.

The task is then to calculate the response function $S(E)$ which describes the removal of a proton from the target nucleus and the formation of the final state, with the ω meson attached to the residual nucleus, and it includes the distorted waves of the incoming deuteron and outgoing ${}^3\text{He}$. The energy variable is $E = T_d + M_d - E_{\text{He}}$ which roughly equals $E_\omega + B_p$, the energy of the produced ω meson plus the binding energy of the removed proton.

The calculation of $S(E)$ is performed using a nuclear shell model with realistic single particle wave functions for the bound proton. Its generic form is [16]

$$S(E) = \frac{1}{\pi} \sum_f \mathcal{F}^\dagger(dp \rightarrow {}^3\text{He}) G_\omega(E - B_p) \mathcal{F}(dp \rightarrow {}^3\text{He}), \quad (12)$$

where the sum is taken over all possible final states that can be reached at given energy transfer E . Here

$$G_\omega(E) = \sum_\lambda |\phi_\lambda\rangle \frac{-2E}{E^2 - E_\lambda^2 + i\epsilon} \langle \phi_\lambda| \quad (13)$$

is the ω meson Green function related to the Klein-Gordon equation (7). The amplitude \mathcal{F} involves the bound proton wave function

$$\Psi_{j_p, l_p}(\vec{r}) = \psi_{j_p l_p}(r) [Y_{l_p}(\hat{r}) \chi_{\frac{1}{2}}]^{[j_p]}. \quad (14)$$

It also involves the distorted waves, $\Psi_i(\vec{p}_d, \vec{r})$ of the incoming deuteron and $\Psi_f(\vec{p}_{He}, \vec{r})$ of the outgoing 3He . Given the high energies of these particle, we can use the eikonal approximation and write (with their momenta \vec{p}_d and \vec{p}_{He} chosen along the z -axis):

$$\Psi_f^\dagger(\vec{p}_{He}, \vec{r}) \Psi_i(\vec{p}_d, \vec{r}) = e^{i(p_d - p_{He})z} D(\vec{r}). \quad (15)$$

We introduce $z = r \cos \Theta$ and the impact parameter $b = \sqrt{x^2 + y^2} = r \sin \Theta$ and write the distortion factor $D(\vec{r})$ as:

$$D(\vec{r}) = \exp \left[-\frac{\sigma_{dN}}{2} \int_{-\infty}^z dz' \rho(z', b) - \frac{\sigma_{{}^3HeN}}{2} \int_z^{\infty} dz' \rho(z', b) \right]. \quad (16)$$

We use $\sigma_{dN} \simeq 83$ mb and $\sigma_{{}^3HeN} \simeq 126$ mb for the deuteron-nucleon and 3He -nucleon cross section at typical beam energies around 4 GeV.

Carrying out all necessary spin and angular momentum sums (including the polarization degrees of freedom of the ω meson) the response function reduces, after some algebra, to the following expression:

$$S(E) = \sum_{j_p, l_p} \sum_{l, L} N_p \frac{2l+1}{4\pi^2} (l_p 0 l 0 | L 0). \quad (17)$$

$$\text{Im} \int_0^\infty dr' r'^2 w_L^*(r') \psi_{j_p l_p}^*(r') \int_0^\infty dr r^2 w_L(r) \psi_{j_p l_p}(r) g_l(E - B_p, r', r),$$

where $\psi_{j_p l_p}$ is the proton radial wave function specified in eq.(14), N_p denotes the number of protons in the specific orbital, and

$$g_l(E; r', r) = 2i E k u_l(k, r_<) v_l^*(k, r_>) \quad (18)$$

is the remaining radial Green function of the ω meson for given angular momentum l , with $r \equiv |\vec{r}|$ and $r' \equiv |\vec{r}'|$. It is written in terms of the regular solution u_l and the outgoing solution v_l^* of the Klein-Gordon equation and applies both for continuum states and for quasi-bound states. The wave number is $k = \sqrt{E^2 - m_\omega^2}$, and bound states are expressed by analytic continuation to imaginary k . Furthermore,

$$w_L(r) = \int_{-1}^1 d\cos \Theta e^{i(p_d - p_{He})r \cos \Theta} D(z(\Theta), b(\Theta)) P_L(\cos \Theta), \quad (19)$$

with Legendre polynomials P_L . Note that the $(d, {}^3He)$ transfer reaction takes place predominantly at the edges of the nuclear target, as shown in Fig.4. The distortion factor causes a suppression of the cross section by typically two orders of magnitude.

Substituting the response function (17) into the cross section (11) we can now study the effects of ω -nuclear binding on the missing energy spectrum measured in the transfer reaction. We choose the case ${}^7Li(d, {}^3He){}_\omega^6He$ as an example, mainly for simplicity of its proton orbital structure and since this choice is referred to in the GSI proposal [8]. The result is shown in Fig.5. The differential cross section is small, but a systematic downward shift of strength as compared to quasi-free ω meson production should be nevertheless visible, even in light nuclei. The effect should be further enhanced in heavier nuclei. The

increased ω meson width in the nuclear environment prohibits a separate identification of isolated bound states, but the overall downward shift of the ${}^3\text{He}$ missing energy spectrum below the free ω meson threshold would indicate the presence of quasi-bound states if they exist. A flat background, not shown here, is expected to come primarily from ρ meson production. The model dependence of the input ωN amplitude is again illustrated by showing results for sets A and B discussed previously. The qualitative conclusions are evidently not much influenced by the difference between these choices. Fig. 5b shows the

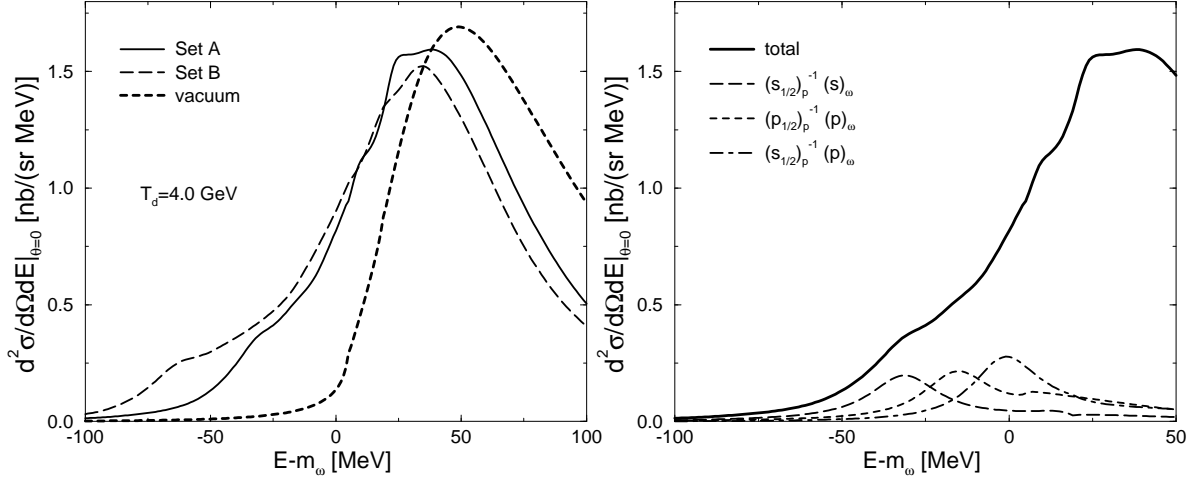


Figure 5: Missing energy spectra of the reaction $d + A \rightarrow {}^3\text{He} + \omega(A - 1)$ at a deuteron kinetic energy $T_d = 4$ GeV in case of $A=7$ (Lithium):

- Cross sections calculated with ω -nuclear potentials, Set A (solid line) and Set B (long dashed line), together with the “vacuum” result (quasi-free ω production, short dashed).
- Separate contributions from transitions of protons of a specified shell (subscript p) to bound states of ω mesons (subscript ω). The total spectrum corresponds to Set A.

decomposition of the quasi-bound spectrum into separate (s - and p -state) orbitals of the ω meson coupled to different proton-hole states.

4.2 Pion-induced ω production

Another interesting option is the $\pi^- p \rightarrow \omega n$ reaction in nuclei [18]. For a neutron emitted in forward direction, a pion with lab. kinetic energy $T_\pi \simeq 2.5$ GeV incident on a proton at rest produces a zero momentum ω meson. For an ω meson bound to a nucleus, $T_\pi \simeq (1.5 - 2)$ GeV may be sufficient. Consider the case in which the ω meson energy E_ω is measured by observing its decay $\omega \rightarrow e^+ e^-$, whereas the emitted neutron remains unobserved. We wish to estimate the differential cross section for this process.

The z -axis of the lab. frame is chosen to coincide with the incoming pion momentum. The cross section is written

$$\frac{d\sigma}{dE_\omega} = \frac{\Gamma_{\omega \rightarrow e^+ e^-}}{\Gamma_{\text{tot}}} \int d\Omega_n \frac{d\sigma_{\pi^- p \rightarrow \omega n}^{\text{Lab}}}{d\Omega_n} \cdot S(E_\omega, \Omega_n), \quad (20)$$

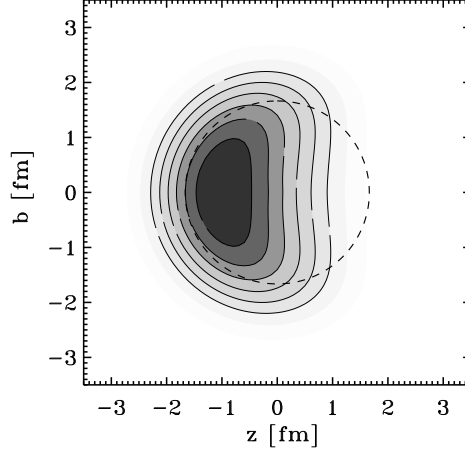


Figure 6: Contour plot of $D(z, b)\rho(r)$ indicating the reaction zone for the $\pi^- A \rightarrow \omega(A-1)$ process on a typical light target nucleus. The dashed curve indicates the r.m.s. radius of the target.

where the integral is taken over the solid angle of the emitted neutron. The factor $\Gamma_{\omega \rightarrow e^+e^-}/\Gamma_{\text{tot}}$ is the branching ratio for the dilepton decay channel of the ω meson, $7.15 \cdot 10^{-5}$ for the free ω and possibly up to an order of magnitude smaller for the in-medium decay. The c.m. cross section for $\pi^- p \rightarrow n\omega$ in free space (see Fig. 7) is almost isotropic and in the range 1-2 mb [17]. One just needs to transform this quantity to the lab frame.

It remains to calculate the response function $S(E_\omega, \Omega_n)$ which now depends on the neutron emission angle. We follow similar steps as in the previous section 4.1. The (undetected) energetic neutron in the final state is treated as a plane wave $\Psi_f(\vec{p}_n, \vec{r}) = \exp(i\vec{p}_n \cdot \vec{r})$. The distorted wave of the incident pion is written

$$\Psi_\pi(p_\pi, \vec{r}) = e^{ip_\pi z} D(\vec{r}), \quad (21)$$

with the distortion factor

$$D(\vec{r}) = \exp \left[-\frac{\sigma_{\pi N}}{2} \int_{-\infty}^z dz' \rho(z', b) \right] \equiv D(z, b). \quad (22)$$

We use $\sigma_{\pi N} \simeq 35$ mb.

Note that the reaction zone is now concentrated in the front hemisphere of the target nucleus (see Fig. 6). The final result for the $\pi^- A \rightarrow \omega(A-1) + n$ response function becomes:

$$S(E_\omega, \Omega_n) = \sum_{j_p, l_p} \sum_{l, L, M} N_p \frac{2l+1}{4\pi^2} (l_p 0 l 0 | L 0) \cdot \quad (23)$$

$$\text{Im} \int_0^\infty dr' r'^2 w_{LM}^*(r', \theta_n) \psi_{j_p l_p}^*(r') \int_0^\infty dr r^2 w_{LM}(r, \theta_n) \psi_{j_p l_p}(r) g_l(E_\omega, r', r),$$

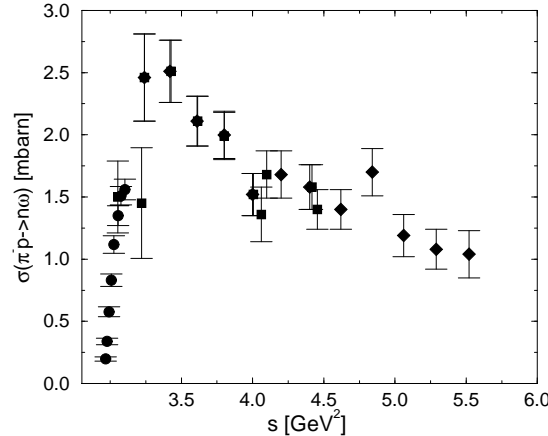


Figure 7: The free cross section of the reaction $\pi^- + p \rightarrow n + \omega$. The data are from ref.[15].

where now ($-L \leq M \leq +L$):

$$w_{LM}(r, \theta_n) = \sqrt{\pi \frac{(L-\mu)!}{(L+\mu)!}} \int_{-1}^1 d\tilde{z} e^{-iz(p_\pi - p_n \cos \theta_n)} D(z, b) P_{L,\mu}(\tilde{z}) I_\mu(p_n b \sin \theta_n), \quad (24)$$

with $\tilde{z} = z/r$, $\mu \equiv |M|$, Legendre functions $P_{L,\mu}$ and Bessel functions I_μ . The remaining integrals are solved numerically.

We show in fig. 8 the expected results for $\pi^- + {}^7\text{Li} \rightarrow {}^6\text{He} + n$ as an example, for the case in which the ω spectrum is detected through e^+e^- pairs. We use set A for the ωN input amplitude. The strong downward shift of the spectral weight in the presence of the ω binding potential is quite apparent, and there are even indications of structures that can be associated with separate quasi-bound orbits of the ω meson. However, the rates are very low. In fact we have used the free $\omega \rightarrow e^+e^-$ branching ratio for normalization, and one expects to loose about an order of magnitude when the in-medium branching ratio is used.

5 Summary and Conclusions

We have investigated the possible formation of quasi-bound ω meson states in nuclei. Such states are indeed predicted to exist if the ω meson (unlike the ρ meson) survives as a quasiparticle in nuclear matter, and if its in-medium mass is shifted downward by more than 10% from its free mass, $m_\omega = 0.78$ GeV, as suggested by several models.

We summarize our results and conclude as follows:

- The complex ω -nuclear potential is expected to be strongly energy dependent, its real part changing from repulsion at low energy to attraction ($\text{Re}U \sim -(100 - 150) \text{ MeV} \cdot \rho/\rho_0$) at $E \sim m_\omega$. This behaviour is consistent with the QCD sum rule analysis of the first moment of the ω meson spectral distribution in nuclear matter.

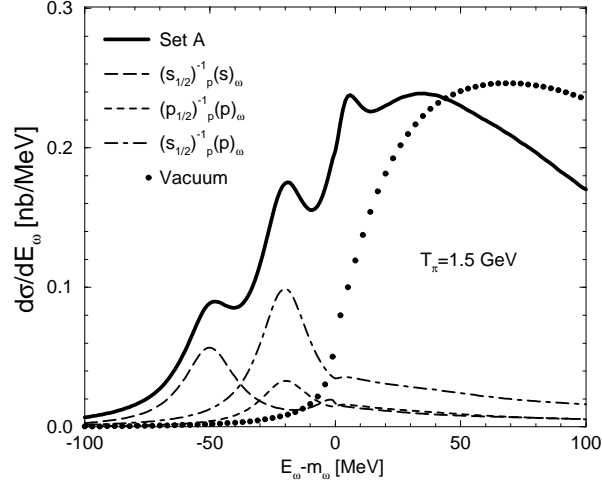


Figure 8: Spectra of the reaction $\pi^- A \rightarrow \omega(A-1) + n$ in case $A = 7$ (Lithium), assuming that the ω meson is detected through its decay into e^+e^- .

Solid line: result with ω -nuclear potential (Set A). Dotted line “vacuum” result (quasi-free ω production). The separate contributions from different bound ω meson orbitals are also shown for comparison.

- The estimated widths of ω -nuclear states in a variety of nuclei with $A \leq 40$ are $\Gamma \lesssim 40$ MeV, up to about five times larger than the free ω decay width. Such widths may prohibit the separate identification of ω -nuclear states in distinct orbitals, but pronounced spectral strength at excitation energies $E < m_\omega$ below the quasifree production threshold should be visible.
- We have examined two possible options for producing ω -nuclear states: ($d, {}^3\text{He}$) transfer reactions and pion-induced formation. The $\pi + A \rightarrow \omega(A-1) + n$ process with subsequent detection of the ω by its decay into e^+e^- is at the borderline of feasibility, with prohibitively low rates. On the other hand, missing energy spectra in $d + A \rightarrow \omega(A-1) + {}^3\text{He}$ reactions look more promising, with forward differential cross sections at the level of nb/(sr·MeV) even for the lightest nuclei. Optimal kinematic conditions would be realized for deuteron beam kinetic energies $T_d \simeq (8-10)$ GeV. Even at $T_d \simeq 4$ GeV the transferred momentum is still well within the range of typical nuclear Fermi momenta.
- The investigation of spectral distributions of ω mesons “at rest” in normal nuclei would be complementary to the search for medium effects on vector meson spectra in high-energy heavy-ion collisions. If such effects are significant at high baryon densities, they should also be seen in less extreme but much better controlled conditions as they are realized in ordinary nuclear systems.

We would like to thank A. Gillitzer, R.S. Hayano, S. Hirenzaki, P. Kienle and H. Toki for fruitful discussions.

References

- [1] E.G. Drukarev and E.M. Levin, Nucl. Phys. **A 511** (1990) 679; Prog. Part. Nucl. Phys. **27** (1991) 77.
- [2] T.D. Cohen, R.J. Furnstahl and D.K. Griegel, Phys. Rev. **C 45**(1992)1881; Phys. Rev. **C 45** (1992) 1881.
- [3] S. Klimt, M. Lutz and W. Weise, Phys. Lett. **B 249** (1990) 386.
- [4] T. Hatsuda and S.H. Lee, Phys. Rev. **C 46** (1992) R34.
- [5] G.E. Brown and M. Rho, Phys. Rev. Lett. **66** (1991) 2720.
- [6] M. Herrmann, B.L. Friman and W. Nörenberg, Nucl. Phys. **A 560** (1993) 411; G. Chanfray and P. Schuck, Nucl. Phys. **A 555** (1993) 329; G. Chanfray, R. Rapp and J. Wambach, Phys. Rev. Lett. **76** (1996) 368.
- [7] F. Klingl, N. Kaiser and W. Weise, Nucl. Phys. **A 624** (1997) 527; F. Klingl and W. Weise, hep-ph/9802211, Acta Phys. Polonica (1998), in print.
- [8] R.S. Hayano, S. Hirenzaki and A. Gillitzer, preprint nucl-th/9806012 (1998); R.S. Hayano et al., GSI-SIS proposal #214 (1997).
- [9] K. Tsushima, D.H. Lu, A.W. Thomas and K. Saito, preprint ADP-98-28/T302; nucl-th/9807028 (1998), Phys. Lett. B (in print).
- [10] F. Klingl, N. Kaiser and W. Weise, Z. Phys. **A 356**(1996)193; N. Kaiser, T. Waas and W. Weise, Nucl. Phys. **A 612** (1997) 297.
- [11] B. Friman, nucl-th9801053, Proc. of the APCTP-workshop on Astro-Hadron Physics, Seoul, Korea, October 1997.
- [12] F. Klingl, Dissertation, TU München (1998).
- [13] F. Klingl and W. Weise, in preparation.
- [14] L.M. Barkov et al., JETP Lett. **46** (1987) 164; S.I. Dolinsky et al., Phys. Reports **202** (1991) 99.
- [15] R. Wurzinger et al., Phys. Rev. **C 51** (1995) R443.
- [16] O. Morimatsu and K. Yazaki, Nucl. Phys. **A 483** (1988) 493; Nucl. Phys. **A 435** (1985) 727; J. Hüfner, S. Y. Lee and H. A. Weidenmüller, Nucl.Phys. **A 234**(1974)42; C.B. Dover, L. Ludeking and G.E. Walker, Phys. Rev. **C 22** (1980) 2073.
- [17] H. Karami et al., Nucl. Phys. **B 154** (1979) 503; A. Baldini, V. Flaminio, W.G. Moorhead and D.R.O. Morrison, Landolt Börnstein **Vol. 12a**, ed. H Schopper (Springer, Berlin, 1988).
- [18] W. Schön, H.Bokemeyer, W. Koenig and V. Metag, Acta Phys. Polonica **B 27** (1996) 2959.

